# Effects of $Ca^{2+}$-Activated Calmodulin on Neuronal Nitric Oxide Synthase Reductase Activity and Binding of Substrates: pH Dependence of Kinetic Parameters†

Kirsten R. Wolthers‡ and Michael I. Schimerlik*,‡,§

*Department of Biochemistry and Biophysics and Environmental Health Sciences Center, Oregon State University, Corvallis, Oregon 97331*

*Received May 8, 2001; Revised Manuscript Received August 29, 2001*

ABSTRACT: The pH dependence of basal and calmodulin- (CaM-) stimulated neuronal nitric oxide synthase (nNOS) reduction of 2,6-dichloroindophenol (DCIP) and cytochrome $c^{3+}$ was investigated. The wave-shaped log *V* versus pH profile revealed that optimal DCIP reduction occurred when a group, p$K_a$ of 7.6−7.8, was ionized. The $(V/K)_{NADPH}$ and $(V/K)_{DCIP}$ versus pH profiles increased with the protonation of a group with a p$K_a$ of 6.5 or 5.9 and the ionization of two groups with the same p$K_a$ of 7.5 or 7.0, respectively. $(V/K)_{DCIP}$ decreased with the ionization of a group, p$K_a$ of 9.0. Similar *V*, $(V/K)_{NADPH}$, and $(V/K)_{DCIP}$ versus pH profiles for DCIP reduction were obtained with and without CaM, indicating that CaM does not influence ionizable groups involved in catalysis or substrate binding. In contrast, CaM affected the pH dependence of cytochrome $c^{3+}$ reduction. The wave-shaped log *V* versus pH profile for basal cytochrome $c^{3+}$ reduction revealed that ionization of a group, p$K_a$ of 8.6, increased catalysis. Log *V* for CaM-stimulated cytochrome $c^{3+}$ reduction displayed a bell-shaped pH dependence with the protonation of a group with a p$K_a$ of 6.4 and the ionization of a group with a p$K_a$ of 9.3, resulting in a loss of activity. The $\log(V/K)_{cytc}$ versus pH profiles with and without CaM were bell-shaped with the ionization of a group at p$K_a$ of 7.1 or 7.6 (CaM) or p$K_a$ of 9.4 or 9.6 (CaM), increasing and decreasing $(V/K)_{cytc}$. These results suggest that CaM may change the nature of the rate-limiting catalytic steps or ionizable groups involved in cytochrome $c^{3+}$ reduction.

The nitric oxide synthases (NOS)[1] are a family of three mammalian isozymes which produce the physiologically important free radical nitric oxide (NO) (for reviews see refs *1*−*5*). Each of the isozymes functions as a homodimer to produce NO and L-citrulline via the five-electron oxidation of L-arginine (*6*, *7*). The polypeptide subunit for each of the three isoforms is divided into two distinct domains. The oxygenase domain contains a P450-type heme and the binding sites for the cofactor (6*R*)-5,6,7,8-tetrahydrobiopterin ($H_4B$) and the substrate L-arginine (*8*−*11*). The reductase domain contains 1 mol each of FAD and FMN and the binding site for NADPH (*12*, *13*). The calmodulin- (CaM-) binding motif, located at the center of each of the NOS polypeptide subunits, tethers the oxygenase domain to the reductase domain (*14*−*16*). A rise in intracellular $Ca^{2+}$ concentrations promotes the binding of CaM to neuronal (nNOS) and endothelial (eNOS) NOS which triggers inter-domain electron transfer, an essential step for NO synthesis (*17*−*19*). In contrast, CaM is tightly bound to the inducible (iNOS) isoform at basal intracellular levels of $Ca^{2+}$; enzyme activity is modulated at the transcriptional level through the action of cytokines (*16*).

The dual flavin-containing domain of NOS is structurally and functionally similar to NADPH−cytochrome P450 reductase (CPR; *12*, *13*). During catalysis, the enzyme-bound flavins on nNOS and CPR cycle between the one- and three-electron reduced states as they shuttle reducing equivalents from NADPH to FAD and then FMN and finally to the heme (*13*, *20*−*23*). CPR and nNOS are both able to reduce the nonphysiological flavin electron acceptors, ferricyanide (FeCN), 2,6-dichloroindophenol (DCIP), and cytochrome $c^{3+}$ (*24*, *25*). The binding of $Ca^{2+}$-activated CaM ($Ca^{2+}$-CaM) to nNOS alleviates the inhibition of flavin-mediated electron transfer, resulting in a 2−3-fold increase in FeCN and DCIP reduction and a 10−20-fold increase in cytochrome $c^{3+}$ reduction (*14*, *17*). Similar levels of $Ca^{2+}$-CaM-induced stimulation of these activities is achieved with the nNOS reductase domain. Thus, this behavior is not attributed to

† This work was supported by Grant ES0040 from the National Institute of Environmental Health Sciences.

* To whom correspondence should be addressed at the Department of Biochemistry and Biophysics, Agricultural and Life Sciences Building 2011, Oregon State University, Corvallis, OR 97331. Telephone: (541) 737-2029. Fax: (541) 737-0481. E-mail: schimerm@onid.orst.edu.

‡ Department of Biochemistry and Biophysics, Oregon State University.

§ Environmental and Health Sciences Center, Oregon State University.

[1] Abbreviations: NOS, nitric oxide synthase; NO, nitric oxide; nNOS, neuronal NOS; eNOS, endothelial NOS; iNOS, inducible NOS; $H_4B$, (6*R*)-5,6,7,8-tetrahydrobiopterin; $Ca^{2+}$-CaM, $Ca^{2+}$-activated calmodulin; CPR, NADPH−cytochrome P450 oxidoreductase; FeCN, ferricyanide; DCIP, 2,6-dichloroindophenol; cyt *c*, cytochrome $c^{3+}$; 2′AMP, 2′-adenosine monophosphate; MES, 2-(*N*-morpholino)ethanesulfonic acid; CHES, 2-(*N*-cyclohexylamino)ethanesulfonic acid; NMR, nuclear magnetic resonance; $DCIP_{ox}$, oxidized form of DCIP; $DCIP_{red}$, reduced form of DCIP.

10.1021/bi010947t CCC: $22.00 
Published on Web 12/08/2001

the cofactor triggering electron transfer to the heme (*17*, *26*, *27*). $Ca^{2+}$-CaM also has a negligible effect on the flavin midpoint potentials; thus, the cofactor does not change the thermodynamic driving force of electron transfer in the reductase domain (*22*). However, $Ca^{2+}$-CaM has been shown to increase the pre-steady-state rate of electron transfer from NADPH to the flavins (*17*) and to induce conformational changes in the diflavin domain (*14*, *23*, *28*).

The binding of $Ca^{2+}$-CaM may remove the suppression of electron transfer by acting on structural components which are absent in CPR. All three NOS isoforms possess 21−40 additional amino acids at the C-terminal tail, and the constitutive isoforms (nNOS and eNOS) contain a 45−50 amino acid insert located in the FMN-binding domain. In the absence of $Ca^{2+}$-CaM, eNOS and nNOS lacking their C-terminal tails exhibit faster rates of flavin and cytochrome $c^{3+}$ reduction compared to wild-type (*29*). The CaM-stimulated cytochrome $c^{3+}$ reductase activity was similar for the wild-type and the truncated forms, suggesting that the C-terminal tail acts to suppress electron transfer which can then be alleviated with the binding of $Ca^{2+}$-CaM (*29*). Removal of the 45−50 amino acid sequence in the FMN domain demonstrated that this is a putative autoinhibitory element as it promotes the dissociation of CaM at low intracellular $Ca^{2+}$ concentrations and inhibits electron transfer in the absence of $Ca^{2+}$-CaM (*30*−*32*).

The NOS isoforms exhibit varying rates of NO synthesis, which is correlated to their rate of interflavin electron transfer and/or transfer between the FMN and the heme (*33*). Because the reductase domain controls the rate of NO production, there is great interest in the role of $Ca^{2+}$-CaM in mediating electron transfer. The steady-state kinetic mechanisms for DCIP and cytochrome $c^{3+}$ reduction were the same in the presence and absence of the activated cofactor. The reduction of DCIP and cytochrome $c^{3+}$ occurs in two half-reactions by a one-site ping-pong and a two-site ping-pong mechanism, respectively (*34*). The role of $Ca^{2+}$-CaM is further investigated in this paper by determining its influence on ionizable groups associated with catalysis or binding of substrates. The pH profile for $V$ yields p$K_a$ values for groups involved in rate-limiting step(s) of the mechanism. In contrast, the p$K_a$ values in the $V/K$ versus pH profiles represent groups in the steady-state mechanism that participate in events from binding of the substrate up to the first irreversible step, which could be a catalytic step or product release. If the p$K_a$ appears in both the $V$ and $V/K$ versus pH profiles, it represents the particular ionization state of a group on the enzyme or substrate that is limiting for catalysis rather than one involved solely in substrate binding (*35*). The proposed steady-state kinetic mechanisms for the reduction of these two substrates provide a framework for the interpretation of the dependence of $V$ and $V/K$ for substrates on pH.

## EXPERIMENTAL PROCEDURES

*Materials.* Hepes was purchased from Research Organics (Cleveland, OH). $H_4B$ was from Cayman Chemical Co. (Ann Arbor, MI). The 2′,5′-ADP−Sepharose was from Amersham Pharmacia Biotech (Piscataway, NJ), and the calmodulin−Sepharose and calmodulin were generous gifts of Dr. S. Anderson (Oregon State University). All other reagents were from Sigma Chemical Co. (St. Louis, MO).

*Protein Expression and Purification*. Recombinant rat nNOS was purified from *Escherichia coli* strain BL21(DE3) after overexpression of the cDNA with the pCWori vector. The enzyme was purified according to the protocol published by Gerber and Ortiz de Montellano with slight modification (*36*). The rate of NO production was measured by the hemoglobin−NO capture assay at 25 °C following the procedures of Stuehr et al. (*37*). nNOS was more than 85% pure as judged by SDS−polyacrylamide gel electrophoresis with a specific activity of 150 nmol of NO $min^{-1}$ $mg^{-1}$ at 25 °C. Protein concentration was determined with the Lowry assay using BSA as a standard (*38*).

*Substrate Titrations.* $^{31}P$ NMR spectra for NADPH titration curves were obtained with a Bruker DRX 600 spectrometer operating at 242.9 MHz using a 90° observation pulse. Experiments were performed at 25 °C using a 5 mm NMR tube. The spectra were collected unlocked with constant compensation for field drift. Titration samples contained 1 mM NADPH in the buffer used for the pH kinetic studies. The spectrophotometric titration of DCIP at 600 nm was performed at 25 °C. The samples contained 20 $\mu$M DCIP in the buffer used for the pH kinetic experiments.

*Measurement of Reductase Activities*. A three-component buffer system consisting of 15 mM MES (p$K_a$ 6.15), 15 mM Hepes (p$K_a$ 7.55), and 15 mM CHES (p$K_a$ 9.5) was used for the pH dependence studies. The buffer was titrated to the desired pH with NaOH. Reactions were performed in a 5.0 mL volume at 25 °C using either a 1 or 5 cm path-length cuvette. The rate of cytochrome $c^{3+}$ reduction was measured by following absorbance changes at 550 nm ($\Delta\epsilon$ = 21.1 $mM^{-1}$ $cm^{-1}$; *39*). The rate of DCIP reduction was measured by following absorbance changes at 600 nm using an extinction coefficient for DCIP that was calculated at each pH (described below). Reaction mixtures contained variable concentrations of substrates (NADPH, cytochrome $c^{3+}$, or DCIP) and, where appropriate, 10 $\mu$M $CaCl_2$ and 100 nM CaM. Reactions were initiated by the addition of 0.5−1.5 $\mu$g of nNOS to a 5 mL reaction volume. The pH profiles were extended as far as possible into the pH extremes until enzyme or substrate instability prevented the measurement of initial rates. At pH values below 7 the level of uncatalyzed NADPH oxidation in the absence of nNOS was subtracted from initial rates obtained in the presence of the enzyme.

*Data Analysis*. Values for the various parameters were derived by nonlinear least-squares fitting (Levenberg−Marquardt algorithm) using the computer program Origin version 4.0 (MicroCal Software Inc., North Hampton, MA) or MicroMath Scientist (MicroMath Scientific Software, Salt Lake City, UT). $V$ and $K_{cytc}$ values for the basal and CaM-stimulated reduction of cytochrome $c^{3+}$ were obtained by measuring the rate of cytochrome $c^{3+}$ reduction at a fixed saturating concentration of NADPH (10 $\mu$M). The initial rates were fit to the Michaelis−Menten equation:

$$v_i = \frac{VA}{K_m + A} \quad (1)$$

where $v_i$ represents the initial rate, $V$ is the maximal velocity, $A$ is the variable substrate concentration, and $K_m$ is the Michaelis constant for the variable substrate. $(V/K)_{cytc}$ was obtained from the fitted values of $V$ and $K_{cytc}$ with the appropriate error propagation. $(V/K)_{NADPH}$ values for the basal

and CaM-stimulated reduction of DCIP were obtained in the same fashion with DCIP present at a constant subsaturating concentration of 20 $\mu$M. Concentrations of NADPH greater than $2K_{NADPH}$ inhibit DCIP reduction at DCIP concentrations less than $K_{DCIP}$; thus, $(V/K)_{DCIP}$ in the presence and absence of $Ca^{2+}$-CaM was determined by fitting the initial rates at various DCIP concentrations at a fixed nonsaturating level of NADPH (0.3 $\mu$M) to eq 1. This method is valid since the basal and CaM-stimulated reduction of DCIP follows a ping-pong mechanism (*34*); therefore, the concentration of the nonvariable substrate can be maintained at nonsaturating levels without affecting the value of *V/K* for the variable substrate. The *V* versus pH profile for basal and CaM-stimulated reduction of DCIP was determined by measuring the initial rate at saturating concentrations of NADPH (20 $\mu$M) and DCIP (100 $\mu$M).

Titration curves for NADPH and DCIP were fit to the equation:

$$Y = \frac{Y_H + Y_L(H/K_a)}{H/K_a + 1} \quad (2)$$

where *Y* is the $^{31}$P NMR chemical shift of NADPH or the extinction coefficient of DCIP, *H* is the proton concentration, $K_a$ is the acid dissociation constant, and $Y_L$ and $Y_H$ are the low- and high-pH plateau values, respectively, for *Y*. All plots of the kinetic data contain error bars for each data point corresponding to one standard deviation. The following equation was used to fit a wave with the ionization of one group leading to an increase in the rate of catalysis (Figure 1 and panel A of Figure 4):

$$\log Y = \log\left[\frac{Y_H + Y_L(H/K_a)}{1 + H/K_a}\right] \quad (3)$$

where *Y* denotes the observed maximal velocity, *H* is the proton concentration, $K_a$ is the acid dissociation constant (listed as $K_{a2}$ for Figure 1 and $K_{a1}$ for panel A of Figure 4), and $Y_H$ and $Y_L$ are the values for *Y* at the high- and low-pH plateaus, respectively. $(V/K)_{NADPH}$ versus pH profiles in which the ionization of a group with a low p$K_a$ decreases $(V/K)_{NADPH}$ and the ionization of two groups with the same p$K_a$ leads to an increase in $(V/K)_{NADPH}$ (Figure 2) were fit to the equation:

$$\log Y = \log\left[\frac{Y_H + Y_L(H/K_{a1})(H/K_{a2})^2}{(1 + H/K_{a1})(1 + H/K_{a2})^2}\right] \quad (4)$$

where *Y* is the observed $(V/K)_{NADPH}$, *H* is the proton concentration, $K_{a1}$ is the acid dissociation constant of the group which ionizes at a lower pH, $K_{a2}$ is the acid dissociation constant for the two groups that ionize at a high pH, and $Y_H$ and $Y_L$ are the values of $(V/K)_{NADPH}$ at the high- and low-pH plateaus, respectively. The $(V/K)_{DCIP}$ versus pH profiles in which the ionization of a group with a low p$K_a$, the protonation of two groups with the same midrange p$K_a$, and the ionization of a group with a high p$K_a$ all lead to a decrease in $(V/K)_{DCIP}$ (Figure 3) were fit to the equation:

$$\log Y = \log\left[\frac{Y_H + Y_L(H/K_{a1})(H/K_{a2})^2}{(1 + H/K_{a1})(1 + H/K_{a2})^2(1 + K_{a3}/H)}\right] \quad (5)$$

where *Y* is the observed $(V/K)_{DCIP}$, $K_{a1}$, $K_{a2}$, and $K_{a3}$ are the dissociation constants for the groups that ionize at low, neutral, and high pH, respectively, and $Y_H$ and $Y_L$ are the high- and low-pH plateau values for *Y*, respectively. Bell-shaped pH profiles where catalysis requires the ionization of a group with a low p$K_a$ and the protonation of a group having a higher p$K_a$ (panel B of Figures 4 and 5) were fit to the equation:

$$\log Y = \log\left[\frac{Y_H}{1 + H/K_{a2} + K_{a1}/H}\right] \quad (6)$$

where *Y* is the observed *V* or $(V/K)_{cytc}$, $K_{a1}$ and $K_{a2}$ are the dissociation constants for the groups that ionize at low and high pH, respectively, and $Y_H$ is the value for *V* or $(V/K)_{cytc}$ when both groups are in their preferred ionization states.

## RESULTS

*Determination of Substrate p$K_a$ Values.* The p$K_a$ values for ionizable groups on NADPH and DCIP were determined to aid in the interpretation of the pH profiles. The pH variation in the chemical shift of $^{31}$P by NMR has been the method previously employed to determine the p$K_a$ of the NADPH 2′-phosphate. The p$K_a$ values were reported to be 6.1 for NADPH in 100% $D_2O$ containing 500 mM KCl at 11 °C (*40*) and 6.52 in 10% $D_2O$ and 10% glycerol at 25 °C (*41*). At an ionic strength of 800 mM and in the absence of $D_2O$, Sem and Kasper reported a p$K_a$ of 5.91 for the 2′-phosphate of NADPH (*42*). From the variation in the above-reported values, it is apparent that both ionic strength and the presence of $D_2O$ will affect the p$K_a$ of the NADPH 2′-phosphate. Therefore, it was necessary to determine the p$K_a$ under the conditions of our pH studies. To avoid the use of $D_2O$ in the buffer, the spectra were collected unlocked with constant compensation for the field drift. At 25 °C the p$K_a$ of the NADPH 2′-phosphate equaled 6.46 ± 0.02 (data not shown).

A DCIP hydroxyl group ionizes in the pH range studied and therefore affects the extinction coefficient for this substrate. The p$K_a$ of this group under the buffering conditions used for the nNOS pH studies was determined by measuring the absorbance of 20 $\mu$M DCIP at various pH values. A nonlinear least-squares fit of the data to eq 2 yielded a p$K_a$ for the hydroxyl group equal to 5.87 ± 0.02 (data not shown), which is identical within error to the value obtained by Sem and Kasper (*42*). The extinction coefficients used for calculating initial rates of DCIP reduction in the pH dependence studies were calculated at each pH using eq 2 and assuming an extinction coefficient of 21.0 $mM^{-1}$ $cm^{-1}$ at pH 7.0 (*43*).

*pH Dependence of the Kinetic Parameters for DCIP Reduction.* The kinetic parameters for the nNOS-catalyzed reduction of DCIP were measured over the pH range of 5.5−9. The p$K_a$ values for *V*, $(V/K)_{NADPH}$, and $(V/K)_{DCIP}$ are listed in Table 1. The log *V* versus pH profiles for the basal and CaM-stimulated reduction of DCIP were wave-shaped with the ionization of a group with a p$K_a$ (p$K_{a2}$) of 7.65 ± 0.06 (basal) or 7.77 ± 0.04 ($Ca^{2+}$-CaM) leading to an increase in the rate of DCIP reduction (Figure 1).

The $(V/K)_{NADPH}$ versus pH profiles for basal and CaM-stimulated DCIP reductase activity are shown Figure 2.

Table 1: pH Dependence of Kinetic Parameters for DCIP Reduction

| kinetic parameter | $Ca^{2+}$-CaM | p$K_{a1}$ | p$K_{a2}$ | p$K_{a3}$ |
|---|---|---|---|---|
| $V$ | − | | 7.65 ± 0.06 | |
| $V$ | + | | 7.77 ± 0.04 | |
| $(V/K)_{NADPH}$ | − | 6.47 ± 0.37 | 7.51 ± 0.07 | |
| $(V/K)_{NADPH}$ | + | 6.47 ± 0.20 | 7.56 ± 0.05 | |
| $(V/K)_{DCIP}$ | − | 5.87[a] | 6.97 ± 0.07 | 9.00 ± 0.22 |
| $(V/K)_{DCIP}$ | + | 5.87[a] | 7.08 ± 0.07 | 9.01 ± 0.21 |

[a] Value was fixed.

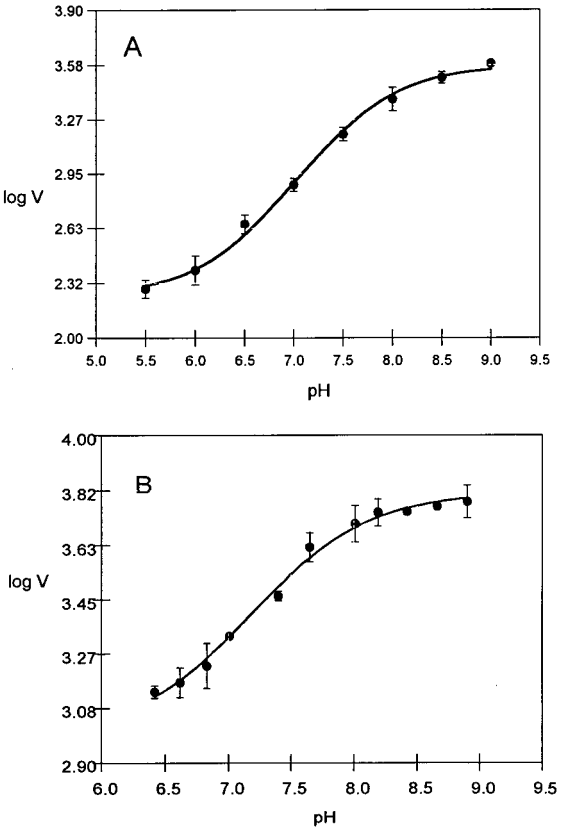


FIGURE 1: pH dependence of log $V$ for the nNOS-catalyzed reduction of DCIP in the (A) absence and (B) presence of 10 $\mu$M $CaCl_2$ and 100 nM CaM. The reaction mixtures also contained 100 $\mu$M DCIP, 20 $\mu$M NADPH, and 1.5 $\mu$g of nNOS. The data points in panels A and B were fit to eq 3, and the p$K_a$ values are listed in Table 1.

$(V/K)_{NADPH}$ increased in the low-pH extreme when a group with a p$K_a$ (p$K_{a1}$) of 6.47 ± 0.37 (basal) or 6.47 ± 0.20 ($Ca^{2+}$-CaM) was protonated. p$K_{a1}$ may reflect the ionization of the 2′-phosphate of NADPH since it equals the p$K_a$ determined in the titration of $^{31}P$ for NADPH and does not appear in the $V$ versus pH profile (Figure 1). The increase in $(V/K)_{NADPH}$ at a low pH suggests that the protonated or monoanionic form of the 2′-phosphate is the preferred state for binding of the nucleotide to nNOS. $(V/K)_{NADPH}$ increases with the ionization of two groups with a p$K_{a2}$ of 7.51 ± 0.07 (basal) or 7.56 ± 0.05 ($Ca^{2+}$-CaM). One of the groups in each profile reflects a group involved in catalysis since a similar p$K_a$ is observed in the $V$ versus pH profile for DCIP reduction.

$(V/K)_{DCIP}$ also increases at low pH (Figure 3). The p$K_a$ for this group, p$K_{a1}$, is shifted to low pH compared to that found for $(V/K)_{NADPH}$. The number of data points was insufficient to obtain an accurate determination of p$K_{a1}$ when

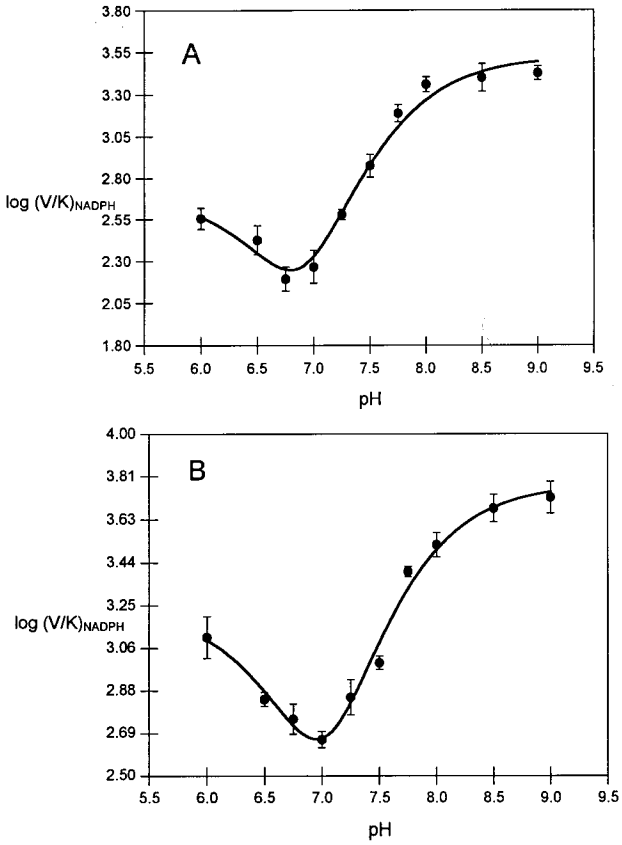


FIGURE 2: pH dependence of log$(V/K)_{NADPH}$ for the nNOS-catalyzed reduction for DCIP in the (A) absence and (B) presence of 10 $\mu$M $CaCl_2$ and 100 nM CaM. The reaction mixtures also contained varying concentrations of NADPH, 20 $\mu$M DCIP, and 0.5 $\mu$g of nNOS. The data in panels A and B were fit to eq 4, and the p$K_a$ values are listed in Table 1.

eq 4 or eq 5 was used to fit the data, and the pH profile could not be extended to lower pH values due to the increase in uncatalyzed NADPH oxidation. If it is assumed that p$K_{a1}$ originates from the ionization of the hydroxyl group on DCIP and p$K_{a1}$ is fixed at 5.87 during the fitting routine, a reasonable fit of the data is obtained using eq 5. The p$K_a$ values for the ionization of two groups resulting in an increase in $(V/K)_{DCIP}$, p$K_{a2}$, were equal with values of 6.97 ± 0.07 (basal) or 7.08 ± 0.07 ($Ca^{2+}$ − CaM). On the basic pH limb, $(V/K)_{DCIP}$ decreased with an ionization of a group, p$K_{a3}$, of 9.00 ± 0.22 (basal) or 9.01 ± 0.21 ($Ca^{2+}$-CaM). A more accurate determination of p$K_{a3}$ could not be obtained because nNOS was unstable at pH >9.0. The value of p$K_{a2}$ is comparable to the p$K_{a2}$ in the $V$ versus pH profile for basal and CaM-stimulated reduction of DCIP (Figure 1). Therefore, it probably reflects an ionizable group involved in catalysis and not the binding of DCIP. However, the other p$K_{a2}$ and p$K_{a3}$ represent ionizable groups on nNOS that affect the binding of DCIP since they only appear in the $(V/K)_{DCIP}$ versus pH profile.

*pH Dependence of the Kinetic Parameters for Cytochrome $c^{3+}$ Reduction*. The p$K_a$ values associated with pH dependence of the steady-state kinetic parameters for cytochrome $c^{3+}$ reduction are summarized in Table 2. The log $V$ versus pH profile for the basal reduction of cytochrome $c^{3+}$ is a wave, where the ionization of a group with a p$K_{a1}$ of 8.60 ± 0.04 leads to optimal cytochrome $c^{3+}$ reductase activity (panel A of Figure 4). In contrast, a plot of log $V$ versus pH

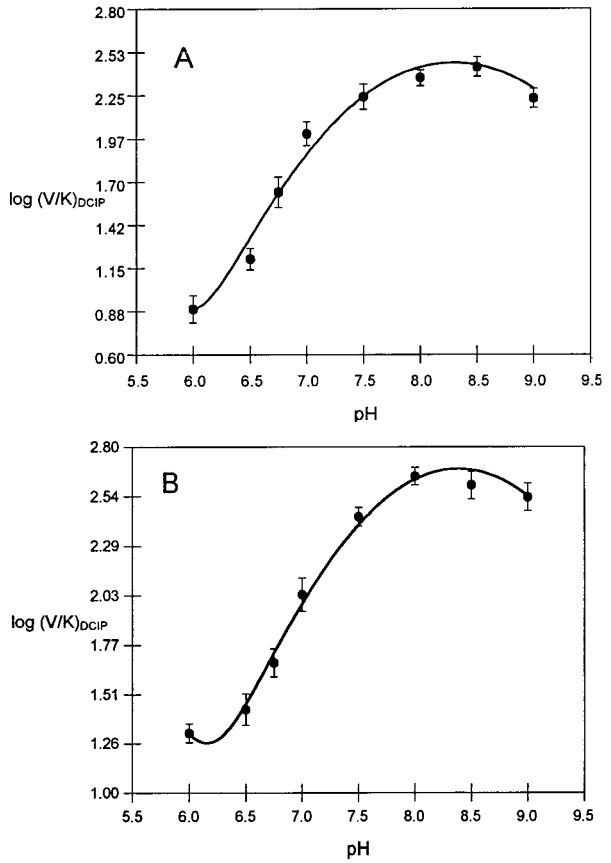


FIGURE 3: pH dependence of log$(V/K)_{DCIP}$ for the nNOS-catalyzed reduction for DCIP in the (A) absence and (B) presence of 10 $\mu$M $CaCl_2$ and 100 nM CaM. The reaction mixtures also contained varying concentrations of DCIP, 0.25 $\mu$M NADPH, and 0.5 $\mu$g of nNOS. The data in A and B were fit to eq 5, and the p$K_a$ values are listed in Table 1.

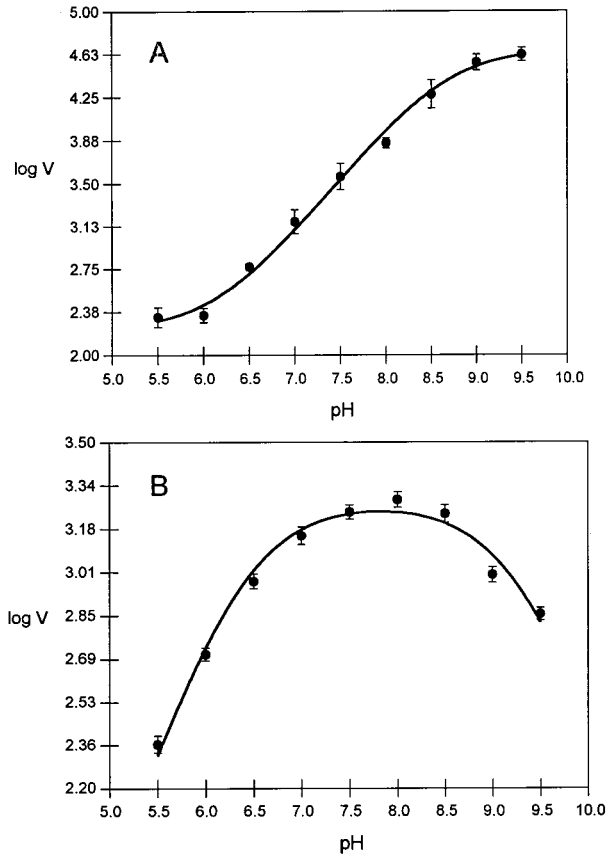


FIGURE 4: pH dependence of log $V$ for the nNOS-catalyzed reduction of cytochrome $c^{3+}$ in the (A) absence and (B) presence of 10 $\mu$M $CaCl_2$ and 100 nM CaM. The reaction mixtures contained varying concentrations of cytochrome $c^{3+}$, 10 $\mu$M NADPH, and 0.5 $\mu$g of nNOS. The data in panel A were fit to eq 3, and the data in panel B were fit to eq 6. The p$K_a$ values are listed in Table 2.

Table 2: pH Dependence of Kinetic Parameters for Cytochrome $c^{3+}$ Reduction

| kinetic parameter | $Ca^{2+}$-CaM | p$K_{a1}$ | p$K_{a2}$ |
|---|---|---|---|
| $V$ | − | 8.60 ± 0.04 | |
| $V$ | + | 6.40 ± 0.06 | 9.25 ± 0.09 |
| $(V/K)_{cytc}$ | − | 7.10 ± 0.12 | 9.38 ± 0.23 |
| $(V/K)_{cytc}$ | + | 7.57 ± 0.12 | 9.62 ± 0.37 |

for the CaM-stimulated reduction of cytochrome $c^{3+}$ forms a bell-shaped curve (panel B of Figure 4). The pH dependence of $V$ shows that the CaM-stimulated activity is dependent on the ionization of a group with a p$K_{a1}$ equal to 6.40 ± 0.06 and the protonation of a group with p$K_{a2}$ equal to 9.25 ± 0.09. Comparison of the pH dependence of $V$ for basal and CaM-stimulated cytochrome $c^{3+}$ reduction indicates that in the presence of $Ca^{2+}$-CaM either two different ionizable groups are involved or p$K_{a1}$ is shifted over 2 pH units and an additional group with a higher p$K_a$ is involved.

The pH variations for $(V/K)_{cytc}$ for the basal and CaM-stimulated reduction of cytochrome $c^{3+}$ are shown in Figure 5. Both profiles show bell-shaped curves, with the ionization of a group with a p$K_{a1}$ of 7.10 ± 0.12 (basal) or 7.58 ± 0.12 ($Ca^{2+}$-CaM) increasing $(V/K)_{cytc}$ and the ionization of a group with a p$K_{a2}$ of 9.38 ± 0.23 (basal) or 9.62 ± 0.37 ($Ca^{2+}$-CaM) resulting in a decrease in $(V/K)_{cytc}$ (Table 2). For the basal cytochrome $c^{3+}$ reductase activity, p$K_{a1}$ shifts from 8.6 in the $V$ versus pH profile to 7.1 in the $(V/K)_{cytc}$ versus pH profile. Since p$K_{a1}$ appears in both profiles, it reflects an ionizable group involved in a catalytic step, and the pH shift could reflect differences in the microenvironment of the cytochrome-free enzyme compared to nNOS complexed with the electron acceptor. p$K_{a2}$ found in the pH dependence of $(V/K)_{cytc}$ for basal cytochrome $c^{3+}$ reduction is not in the corresponding $V$ versus pH profile; thus, the ionization of this group results in a decrease in the binding of cytochrome $c^{3+}$. For CaM-stimulated cytochrome $c^{3+}$ reduction, the two ionizable groups appear in both the bell-shaped log $V$ and log$(V/K)_{cytc}$ versus pH profiles; thus, they represent groups involved in catalysis. The outward shift of the p$K_{a1}$ value from the $V$ to $(V/K)_{cytc}$ versus pH profile by 1.2 pH units possibly reflects a slow substrate release step or solvent exclusion from the active site.

## DISCUSSION

*Interpretation of the pH Profiles for the Reduction of DCIP*. The pH profiles for the substrates DCIP and cytochrome $c^{3+}$ will be interpreted in terms of their previously proposed kinetic mechanisms (*34*). Initial velocity and inhibition studies were consistent with DCIP reduction in the presence and absence of $Ca^{2+}$-CaM following a ping-pong bi-bi mechanism shown in Figure 6. The rate equation for the mechanism drawn in Figure 6, assuming that the binding of substrates/inhibitors and the release of products

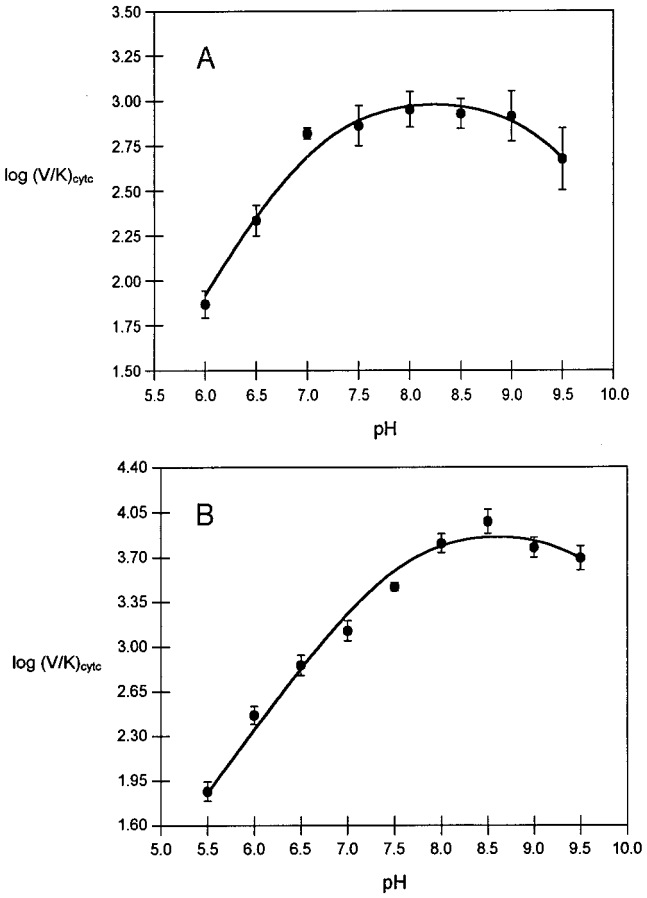


FIGURE 5: pH dependence of $\log(V/K)_{cytc}$ for the nNOS-catalyzed reduction of cytochrome $c^{3+}$ in the (A) absence and (B) presence of 10 $\mu$M $CaCl_2$ and 100 nM CaM. The reaction mixtures contained varying concentrations of cytochrome $c^{3+}$, 10 $\mu$M NADPH, and 0.5 $\mu$g of nNOS. The data in panels A and B were fit to eq 6, and the p$K_a$ values are listed in Table 2.

occurs in rapid equilibrium, gives the following expressions for $V$ and the Michaelis constants for NADPH and DCIP:

$$\frac{V}{E_t} = \frac{k_3k_7k_{11}}{k_3k_7 + k_3k_{11} + k_7k_{11}} \quad (7)$$

$$K_A = \frac{K_{iA}(k_7k_{11})(1 + 1/K)}{k_3k_7 + k_3k_{11} + k_7k_{11}} \quad (8)$$

$$K_B = \frac{K_{iB}(k_3k_7 + k_3k_8)}{k_3k_7 + k_3k_{11} + k_7k_{11}} \quad (9)$$

$V$ is the maximal velocity, $E_t$ is the nNOS concentration, $K_A$ and $K_B$ are the Michaelis constants for NADPH and DCIP, respectively, and $K_{iA}$ and $K_{iB}$ are their corresponding dissociation constants. The rate constants are shown in Figure 6, and $K$ (equal to $E_1/E_1'$) is the equilibrium constant for the conversion of the two free enzyme forms.

The log $V$ versus pH profile for the basal and CaM-stimulated reduction of DCIP is a wave where the ionization of a group with a p$K_{a1}$ of 7.5−7.6 leads to an increase in catalysis (Figure 1). The rate of catalysis reaches a plateau at high and low pH; therefore, it follows the simplified mechanism shown in Scheme 1 where the proton can associate with either the substrate-free or substrate−enzyme binary complex, and both the ionized and protonated forms

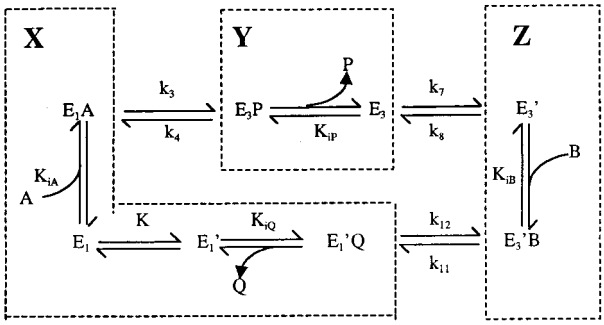


FIGURE 6: Kinetic scheme for a ping-pong bi-bi mechanism for the nNOS-catalyzed reduction of DCIP. A, B, P, and Q represent NADPH, $DCIP_{ox}$, $NADP^+$, and $DCIP_{red}$, and the $K_i$ values refer to their respective dissociation constants. $E_1$ and $E_1'$ are the one-electron (FAD/FMNH$^\bullet$) forms of nNOS that exclusively bind NADPH and 2′AMP, respectively. $E_3$ and $E_3'$ are the three-electron ($FADH^\bullet/FMNH_2$ or $FADH_2/FMNH^\bullet$) forms of nNOS that exclusively bind $NADP^+$ and $DCIP_{ox}$, respectively. $K$ is the equilibrium constant for the conversion of the two enzyme forms, $E_1$ and $E_1'$.

Scheme 1

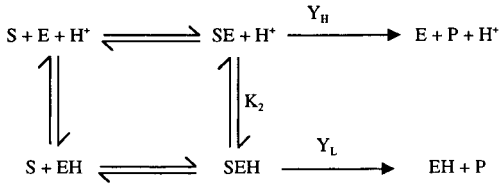


of nNOS are catalytically active. Plots of the pH dependence of $V$ may show changes to a new plateau level when ionization of a group increases the rate of the step that is normally rate limiting (*44*). The basal reduction of DCIP exhibits an ~20-fold difference in the high- and low-pH plateau values for $V$ while the CaM-stimulated activity increases ~7-fold from low to high pH. This suggests that the ionizable step is more rate determining for the basal activity. According to eq 7, the ionization of a group that leads to an increase in a rate-limiting step may be associated with hydride transfer, $k_3$, the steady-state isomerization of $E_3$ to $E_3'$, $k_7$, and/or the rate of electron transfer to DCIP, $k_{11}$.

To determine which of the rate constants may be affected by pH, the $\log(V/K)_{NADPH}$ and the $\log(V/K)_{DCIP}$ versus pH profiles were investigated. $(V/K)_{NADPH}$ and $(V/K)_{DCIP}$ are defined by the following rate and equilibrium constants:

$$\left(\frac{V/E_t}{K_A}\right)_{NADPH} = \frac{k_3}{K_{iA}(1 + 1/K)} \quad (10)$$

$$\left(\frac{V/E_t}{K_B}\right)_{DCIP} = \frac{k_7k_{11}}{K_{iB}(k_7 + k_8)} \quad (11)$$

The $(V/K)_{NADPH}$ versus pH profiles with and without $Ca^{2+}$-CaM were similar in shape (Figure 2). On the acidic limb, $(V/K)_{NADPH}$ increased due to the protonation of a group with a p$K_{a1}$ of 6.47. As the pH became more basic, ionization of two groups with a p$K_{a2}$ of 7.5−7.6 increased the value observed for $(V/K)_{NADPH}$. The ionization of one of these groups is responsible for an accelerated rate of catalysis, since the same p$K_{a2}$ value also appears in the $V$ versus pH profile. Since $k_3$ is the only catalytic rate constant which appears in

$(V/K)_{NADPH}$ (eq 10), the p$K_{a2}$ of 7.5−7.6 which appears in the both the $V$ and $(V/K)_{NADPH}$ versus pH profiles may represent a group whose ionization status affects the rate of hydride transfer. If $k_3$ is slow, or rate limiting compared to $k_7$ and $k_{11}$, then $V$ is largely dependent on $k_3$.

Stopped-flow experiments have shown that $Ca^{2+}$-CaM increases the rate of flavin reduction at 485 nm (*29*). Assuming this signal corresponds to $k_3$, the rate of hydride transfer to FAD, these results may explain the difference in plateau values for basal DCIP reduction (20-fold) compared to CaM-stimulated DCIP reduction (7-fold). If $Ca^{2+}$-CaM stimulates DCIP reduction by increasing $k_3$, which is rate limiting and affected by pH, then the ratio between the high- and low-pH plateaus is expected to be smaller, because $k_3$ would become less rate determining in the presence of the activated cofactor.

The second group with a p$K_{a2}$ of 7.5−7.6 and the group with a p$K_{a1}$ of 6.47 in the $(V/K)_{NADPH}$ versus pH profile (Figure 2) affect the binding of the nucleotide since they do not appear in a plot of $V$ versus pH for DCIP reduction (Figure 1). The value of 6.47 for p$K_{a1}$ was also observed in the titration of the NADPH 2′-phosphate, suggesting that p$K_{a1}$ originates from the nucleotide. If this were the case, then the monoanionic form of the 2′-phospahate of NADPH preferentially binds nNOS. This result is in contrast to a number of other nicotinamide-binding enzymes including CPR (*42*), isocitrate dehydrogenase (*41*), dihydrofolate reductase (*45*), and glyceraldehyde-3-phosphate dehydrogenase (*46*) in which the dianionic form of NADPH preferentially binds. NADPH complexed with these enzymes typically exhibits a lower p$K_a$ value (5−5.5) for the 2′-phosphate, possibly as a result of interactions with positively charged groups in the active site or distortion of the O−P−O angles (*46*). The dianionic form of NADPH may also bind to nNOS, and the p$K_a$ of the 2′-phosphate may be shifted to a lower pH value comparable to the above nucleotide-binding enzymes, such that it is not observed in the $(V/K)_{NADPH}$ versus pH profiles. If this were true, the group with a p$K_{a1}$ of 6.47 would belong to nNOS. The second group with a p$K_{a2}$ of 7.5−7.6 affects the binding of the nucleotide since it only appears in the $(V/K)_{NADPH}$ versus pH profile and not in the pH dependence of $V$.

The amino acid sequence of the NOS NADPH/FAD binding motif in the reductase domain is similar to a class of flavoproteins, the transhydrogenases, which include ferridoxin−$NADP^+$ reductase (FNR), CPR, NADH−nitrate reductase, NADH−cytochrome $b_5$ reductase, and phthalate dioxygenase reductase (*47*). The three-dimensional structure of the FNR• 2′-phosphate−AMP complex shows interaction between the 2′-phosphate and residues Ser234, Arg235, Tyr236, and possibly Lys224 (*48*). These conserved residues have also been implicated in binding the 2′-phosphate of NADPH in other members of the transhydrogenase family. The corresponding residues in nNOS, Ser1313, Arg1314, Lys1320, and Tyr1322, may also play a role in stabilizing the 2′-phosphate. Site-directed mutagenesis combined with pH studies identified Arg597 on CPR with a p$K_a$ of 9.5 as a residue involved in ionic interactions with the 2′-phosphate of NADPH (*49*). The $(V/K)_{NADPH}$ versus pH profile for nNOS could not be extended beyond 9.0 due to enzyme instability, preventing observation of a similar p$K_a$ value at high pH. Assignment of these residues in stabilizing NADPH in nNOS awaits the three-dimensional crystal structure of the enzyme and/or site-directed mutagenesis of these residues.

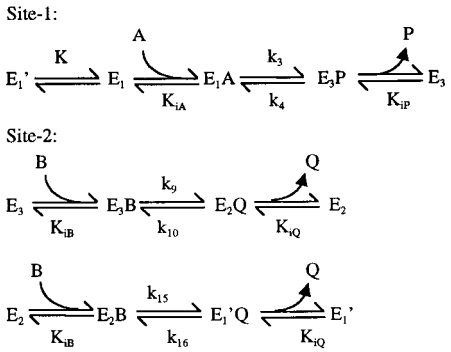


FIGURE 7: Kinetic scheme illustrating the (two-site) ping-pong mechanism for the nNOS-catalyzed reduction of cytochrome $c^{3+}$. A, B, P, and Q represent NADPH, cytochrome $c^{3+}$, $NADP^+$, and cytochrome $c^{2+}$, respectively. $E_1$ and $E_1'$ are the one-electron (FAD/$FMNH^•$) forms of nNOS that exclusively bind NADPH and 2′AMP, respectively. $E_2$ and $E_3$ represent two- (FAD/$FMNH_2$) and three-electron ($FADH^•$/$FMNH_2$) reduced forms of nNOS. $K$ is the equilibrium constant for the conversion of the two enzyme forms, $E_1$ and $E_1'$.

The pH profiles for $(V/K)_{DCIP}$ (Figure 3) and $(V/K)_{NADPH}$ (Figure 2) are similar in that $(V/K)_{DCIP}$ increases at the low-pH limit. A fit of the data in Figure 3 to eq 4 or eq 5 does not generate a defined value for this p$K_{a1}$ because of an inability to obtain data at lower pH values. If we assume that p$K_{a1}$ originates from the ionization of the DCIP hydroxyl and fix this parameter at 5.87, then the remaining parameters can be calculated from eq 5. Studies on CPR-catalyzed reduction of DCIP revealed that $(V/K)_{DCIP}$ decreases at low pH as a group with a p$K_a$ of 5.9, corresponding to the DCIP hydroxyl, is protonated (*42*). In contrast, an increase in $(V/K)_{DCIP}$ in both the basal and CaM-stimulated activities of nNOS indicates that the protonated form of DCIP has a higher affinity for nNOS. If this p$K_a$ corresponds to the DCIP hydroxyl group, the difference in the nNOS and CPR $(V/K)_{DCIP}$ versus pH profiles at acidic pH may be attributed to the two enzymes having different binding sites for DCIP. This may also explain why nNOS depleted of FMN can reduce DCIP (*23*), while CPR cannot (*20*). Alternatively, p$K_{a1}$ may originate from a group on nNOS that facilitates DCIP binding.

A fit of the data in Figure 3 to eq 5 gave p$K_{a2}$ values for the ionization of two groups ranging between 6.9 and 7.1 and a p$K_{a3}$ of 8.8−9.2 for the ionization of a third group. The presence of $Ca^{2+}$-CaM did not significantly influence the p$K_a$ values. According to eq 11, these p$K_a$ values may be a function of ionization equilibria affecting (1) steady-state isomerization of $E_3$ to $E_3'$, $k_7$ and $k_8$, (2) the binding of DCIP, $K_{iB}$, or (3) the rate of electron transfer from the flavins to nNOS, $k_{11}$.

*Interpretation of the pH Profiles for Cytochrome $c^{3+}$ Reductase Activity*. Steady-state kinetic data for basal and CaM-stimulated reduction of cytochrome $c^{3+}$ are consistent with the two-site ping-pong mechanism shown in Figure 7 (*34*). Equations 12−14 are expressions for $V$ and the Michaelis constants for NADPH and cytochrome $c^{3+}$ derived from the rate equation for the mechanism shown in Figure 7, assuming the binding of substrates/inhibitors and the release of products occur in rapid equilibrium.

$$V/E_t = \frac{k_3k_9k_{15}}{k_3k_9 + k_3k_{15} + k_9k_{15}} \quad (12)$$

$$K_A = \frac{(K_{iA})(k_9k_{15})(1 + 1/K)}{k_3k_9 + k_3k_{15} + k_9k_{15}} \quad (13)$$

$$K_B = \frac{(K_{iB})(k_3k_{15} + k_3k_9)}{k_3k_9 + k_3k_{15} + k_9k_{15}} \quad (14)$$

$K_A$ and $K_B$ are the Michaelis constants for NADPH and cytochrome $c^{3+}$ and $K_{iA}$ and $K_{iB}$ are their corresponding dissociation constants. The rate constants are shown in Figure 7, and $K$ (equal to $E_1/E_1'$) is the equilibrium constant for the conversion of the two free enzyme forms.

The log $V$ versus pH profile for the basal cytochrome $c^{3+}$ reductase activity is a wave where the ionization of a group with a p$K_{a1}$ of 8.6 increases catalysis (panel A of Figure 4). The difference between the high- and low-pH plateau values is ~280-fold, indicating that the pH-sensitive step is more rate-determining for basal cytochrome $c^{3+}$ reduction than that observed for DCIP reduction (*44*). According to eq 12, the rate-limiting catalytic step is either hydride transfer, $k_3$, or electron transfer from FMN to cytochrome $c^{3+}$, $k_9$, $k_{15}$.

The pH dependence of cytochrome $c^{3+}$ reduction is dramatically altered in the presence of $Ca^{2+}$-CaM as the log $V$ versus pH profile (panel B of Figure 4) is bell shaped with catalysis dependent on the deprotonation of an acidic group with a p$K_{a1}$ of 6.40 and protonation of basic group with a p$K_{a2}$ of 9.25. The binding of $Ca^{2+}$-CaM may affect the pH profile by changing the rate-limiting step(s). For example, if the rate of hydride transfer is slower than electron transfer from the flavins to cytochrome $c^{3+}$ ($k_3 < k_9$, $k_{15}$), then the p$K_{a1}$ observed in the $V$ versus pH profile for the basal cytochrome $c^{3+}$ reductase activity will reflect the pH dependence of the former step. The increased rate of $k_3$ with respect to $k_9$ and $k_{15}$, induced by the binding of $Ca^{2+}$-CaM, could potentially shift p$K_{a1}$ from 8.60 to 6.40. Alternatively, the conformational changes associated with the binding of $Ca^{2+}$-CaM may change the ionizable groups on nNOS that participate in hydride transfer or electron transfer from FMN to cytochrome $c^{3+}$.

Candidates for ionizable residues on nNOS that could participate in hydride transfer include Cys1348, Ser1177, and Asp1407. The three-dimensional crystal structures of FNR and CPR reveal that these conserved residues are close to the FAD isoalloxazine ring. Substitution of the corresponding cysteine in CPR (Cys630) to an alanine shifted the p$K_a$ of a ionizable group necessary for catalysis from 6.9 to 7.8, indicating that it may be a proton donor/acceptor to the FAD prosthetic group. The corresponding residue in nNOS (Cys1349) is in the putative NADPH−adenine binding motif, adjacent in primary sequence to the C-terminal tail, which has been shown to inhibit electron transfer to FAD in the absence of $Ca^{2+}$-CaM (*29*). The C-terminal tail may affect the location of the Cys1349, Ser1176, and/or Asp1393 by distancing these residues from the FAD, causing them to be ineffective in hydride transfer. This may explain the different p$K_a$ values observed in the $V$ versus pH profiles for cytochrome $c^{3+}$ in the presence and absence of $Ca^{2+}$-CaM.

Alternatively, the p$K_a$ values exhibited in these profiles may originate from the flavins themselves, which exhibit p$K_a$ values in the range studied and are known to be perturbed dramatically with changes in flavin redox state or when the flavins are protein bound (*50*, *51*). Since $Ca^{2+}$-CaM has been shown to induce a conformational change in the FMN-binding domain, the shift in the p$K_a$ may reflect a change in the local environment of flavin within the protein.

The ability of $Ca^{2+}$-CaM to shift the p$K_a$ in the $V$ versus pH profiles for cytochrome $c^{3+}$ and not DCIP may be related to the catalytic mechanism by which nNOS reduces these two substrates. nNOS depleted of its FMN cofactor is still able to reduce DCIP, while it cannot reduce cytochrome $c^{3+}$ (23), indicating that the former substrate is reduced by FAD while the FMN cofactor transfers electrons to cytochrome $c^{3+}$. The binding of $Ca^{2+}$-CaM may be directly affecting the pH dependence of $V$ by acting upon the p$K_a$ of FMN or a neighboring residue and facilitating faster electron transfer at physiological pH.

The pH dependence of $(V/K)_{cytc}$ (Figure 5) was also investigated for basal and CaM-stimulated reduction of cytochrome $c^{3+}$. Both profiles showed that $(V/K)_{cytc}$ increased with the ionization of an acidic group with a p$K_{a1}$ of 7.10 (basal) or 7.57 ($Ca^{2+}$-CaM) and decreased when a group with a p$K_{a2}$ of 9.38 (basal) or 9.62 ($Ca^{2+}$-CaM) ionized. According to eq 15, the expression for $(V/K)_{cytc}$, the p$K_a$ values observed in these pH profiles may reflect groups on nNOS, whose ionization status affects the rates of electron transfer from FMN to cytochrome $c^{3+}$, $k_9$ and $k_{15}$, or the binding of cytochrome $c^{3+}$, $K_{iB}$:

$$\frac{V/E_t}{K_B} = \frac{k_9k_{15}}{(K_{iB})(k_{15} + k_9)} \quad (15)$$

The two ionizable groups in the $(V/K)_{cytc}$ versus pH profile (panel B of Figure 5) also appear in the pH dependence of $V$ (panel B of Figure 4) for the CaM-stimulated reduction of cytochrome $c^{3+}$, indicating that they are not involved in binding of the substrate. Thus, they represent groups involved in electron transfer from the flavins to cytochrome $c^{3+}$, $k_9$ and/or $k_{15}$. The outward displacement of p$K_{a1}$ by 1.2 pH units from a plot of $(V/K)_{cytc}$ versus pH (p$K_{a1}$ = 7.57) to the $V$ versus pH profile (p$K_{a1}$ = 6.40) for CaM-stimulated cytochrome $c^{3+}$ may indicate that $k_3$ is partially rate-limiting such that it affects the observed p$K_{a1}$ value observed in the pH dependence of $V$. Alternatively, the shift in p$K_{a1}$ may be attributed to differences in the microenvironment of cytochrome $c^{3+}$-free nNOS compared to the cytochrome $c^{3+}$−nNOS complex (i.e., solvent exclusion; *44*). Sem and Kasper also noted a 1 pH unit perturbation (7.23 to 6.21) from the $(V/K)_{cytc}$ to $V$ versus pH profiles for CPR reduction of cytochrome $c^{3+}$(*42*). Interestingly, the two enzymes exhibit the same pH profiles when they elicit similar kinetic mechanisms (two-site ping-pong) and turnover rates. The former occurs when the steady-state kinetic analysis of CPR−cytochrome $c^{3+}$ reductase is performed in high ionic strength (850 mM), and the latter occurs when the nNOS cytochrome $c^{3+}$ reductase activity is stimulated by $Ca^{2+}$-CaM.

The p$K_{a2}$ of 9.38, appearing in the $(V/K)_{cytc}$ versus pH profile (panel A of Figure 5), is not present in the $V$ versus pH profile (panel A of Figure 4) for basal cytochrome $c^{3+}$ reduction, indicating that this residue is involved in the binding of cytochrome $c^{3+}$. The ionizable group may

originate from cytochrome $c^{3+}$, which is known to have several lysine residues involved in binding interactions with other enzymes including CPR (46). The corresponding p$K_{a2}$ may not occur in the $(V/K)_{cytc}$ versus pH profile for CaM-stimulated cytochrome $c^{3+}$ reduction because the group ionizes at high pH, and it is difficult to resolve two ionizable groups versus one ionizable group in this region. Alternatively, $Ca^{2+}$-CaM may induce a conformational change such that this ionizable group no longer participates in the binding interaction between cytochrome $c^{3+}$ and nNOS.

In summary, $V$ for basal and CaM-stimulated reduction of DCIP is optimized as a group ionizes with a p$K_{a2}$ of 7.5. This same p$K_{a2}$ appears in the $(V/K)_{NADPH}$ versus pH profile, indicating that the rate-determining step for this kinetic mechanism is hydride transfer from NADPH to FAD. Additional p$K_a$ values appearing in both the $(V/K)_{NADPH}$ and $(V/K)_{DCIP}$ versus pH profiles are ionizable groups that participate in the binding of these two substrates. The presence of $Ca^{2+}$-CaM does not significantly change the p$K_a$ values observed in pH dependence profiles for DCIP, indicating that the presence of the activated cofactor does not affect the nature of the rate-limiting step nor does it alter the groups involved in binding of that substrate. In contrast, $Ca^{2+}$-CaM dramatically affects the pH dependence of $V$ for the reduction of cytochrome $c^{3+}$. The activated cofactor may alter the ionizable groups involved in catalysis, the p$K_a$ values of the flavin cofactors, or the steps that are rate limiting in the kinetic mechanism. It would be of interest to determine the identity of these ionizable groups. This information might be accessible directly from structural analysis or by conducting similar pH studies on nNOS mutants lacking the autoinhibitory domain or the C-terminal tail or the enzyme bound to different flavin analogues.

## ACKNOWLEDGMENT

We are grateful to Drs. Sonia Anderson and Dean Malencik for supplying CaM and the CaM−Sepharose column and to Dr. Ted Dawson for giving us the cDNA plasmid construct for rat neuronal NOS. We thank Dr. Victor Hsu and Joshua Hicks for performing the NMR studies. We also acknowledge the Nucleic Acids and Proteins Core Facilities of Oregon State University Environmental Health Sciences Center in conducting these studies.

## REFERENCES

1. Moncada, S., and Higgs, E. A. (1991) *Eur. J. Clin. Invest. 21*, 361−374.
2. Garthwaite, J., and Boulton, C. L. (1995*) Annu. Rev. Physiol. 57*, 683−706.
3. Marletta, M. A., Tayeh, M. A., and Hevel, J. M. (1990) *Biofactors 2*, 219−225.
4. Nathan, C., and Xie, Q. W. (1994) *Cell 78*, 915−918.
5. Stuehr, D. J., and Griffith, O. W. (1992) *Adv. Enzymol. Relat. Areas Mol. Biol. 65*, 287−346.
6. Knowles, R. G., and Moncada, S. (1994) *Biochem. J. 298*, 249−258.
7. Marletta, M. A. (1994) *Cell 78*, 927−930.
8. Nishimura, J. S., Martasek, P., McMillan, K., Salerno, J., Liu, Q., Gross, S. S., and Masters, B. S. (1995) *Biochem. Biophys. Res. Commun. 210*, 288−294.
9. White, K. A., and Marletta, M. A. (1992) *Biochemistry 31*, 6627−6631.
10. McMillan, K., Bredt, D. S., Hirsch, D. J., Snyder, S. H., Clark, J. E., and Masters, B. S. (1992) *Proc. Natl. Acad. Sci. U.S.A. 89*, 11141−11145.
11. Crane, B. R., Arvai, A. S., Gachhui, R., Wu, C., Ghosh, D. K., Getzoff, E. D., Stuehr, D. J., and Tainer, J. A. (1997) *Science 278*, 425−431.
12. Hevel, J. M., White, K. A., and Marletta, M. A. (1991) *J. Biol. Chem. 266*, 22789−22791.
13. Bredt, D. S., Hwang, P. M., Glatt, C. E., Lowenstein, C., Reed, R. R., and Snyder, S. H. (1991) *Nature 351*, 714−718.
14. Sheta, E. A., McMillan, K., and Masters, B. S. (1994) *J. Biol. Chem. 269*, 15147−15153.
15. Bredt, D. S., and Snyder, S. H. (1990) *Proc. Natl. Acad. Sci. U.S.A. 87*, 682−685.
16. Cho, H. J., Xie, Q. W., Calaycay, J., Mumford, R. A., Swiderek, K. M., Lee, T. D., and Nathan, C. (1992) *J. Exp. Med. 176*, 599−604.
17. Abu-Soud, H. M., Yoho, L. L., and Stuehr, D. J. (1994) *J. Biol. Chem. 269*, 32047−32050.
18. Abu-Soud, H. M., and Stuehr, D. J. (1993) *Proc. Natl. Acad. Sci. U.S.A. 90*, 10769−10772.
19. Schmidt, H. H., Pollock, J. S., Nakane, M., Gorsky, L. D., Forstermann, U., and Murad, F. (1991) *Proc. Natl. Acad. Sci. U.S.A. 88*, 365−369.
20. Iyanagi, T., Makino, N., and Mason, H. S. (1974) *Biochemistry 13*, 1701−1710.
21. Vermilion, J. L., and Coon, M. L. (1978) *J. Biol. Chem. 253*, 8812−8819.
22. Noble, M. A., Munro, A. W., Rivers, S. L., Robledo, L., Daff, S. N., Yellowlees, L. J., Shimizu, T., Sagami, I., Guillemette, J. G., and Chapman, S. K. (1999) *Biochemistry 38*, 16413−16418.
23. Adak, S., Ghosh, S., Abu-Soud, H. M., and Stuehr, D. J. (1999) *J. Biol. Chem. 274*, 22313−22320.
24. Klatt, P., Heinzel, B., John, M., Kastner, M., Bohme, E., and Mayer, B. (1992) *J. Biol. Chem. 267*, 11374−11378.
25. Williams, C. H. J., and Kamin, H. (1962) *J. Biol. Chem. 237*, 587−595.
26. Wolff, D. J., Datto, G. A., Samatovicz, R. A., and Tempsick, R. A. (1993) *J. Biol. Chem. 268*, 9425−9429.
27. Gachhui, R., Ghosh, D. K., Wu, C., Parkinson, J., Crane, B. R., and Stuehr, D. J. (1997) *Biochemistry 36*, 5097−5103.
28. Gachhui, R., Presta, A., Bentley, D. F., Abu-Soud, H. M., McArthur, R., Brudvig, G., Ghosh, D. K., and Stuehr, D. J. (1996) *J. Biol. Chem. 271*, 20594−20602.
29. Roman, L. J., Martasek, P., Miller, R. T., Harris, D. E., de la Garza, M. A., Shea, T. M., Kim, J., and Siler Masters, B. S. (2000) *J. Biol. Chem. 275*, 29225−29232.
30. Salerno, J. C., Harris, D. E., Irizarry, K., Patel, B., Morales, A. J., Smith, S. M., Martasek, P., Roman, L. J., Masters, B. S., Jones, C. L., Weissman, B. A., Lane, P., Liu, Q., and Gross, S. S. (1997) *J. Biol. Chem. 272*, 29769−29777.
31. Daff, S., Sagami, I., and Shimizu, T. (1999) *J. Biol. Chem. 274*, 30589−30595.
32. Chen, P., and Wu, K. K. (2000) *J. Biol. Chem. 275*, 13155−13163.
33. Nishida, C. R., and Ortiz de Montellano, P. R. (1998) *J. Biol. Chem. 273*, 5566−5571.
34. Wolthers, K. R., and Schimerlik, M. I. (2001) *Biochemistry 40*, 4722−4737.
35. Cleland, W. W. (1982) *Methods Enzymol. 87*, 390−405.
36. Gerber, N. C., and Ortiz de Montellano, P. R. (1995) *J. Biol. Chem. 270*, 17791−17796.
37. Stuehr, D. J., Cho, H. J., Kwon, N. S., Weise, M. F., and Nathan, C. F. (1991) *Proc. Natl. Acad. Sci. U.S.A. 88*, 7773−7777.
38. Peterson, G. (1977) *Anal. Biochem. 83*, 346−356.
39. Gelder, B. F. V., and Slater, E. C. (1962) *Biochim. Biophys. Acta 58*, 593−595.
40. Feeney, J., Birdsall, B., Roberts, G. C., and Burgen, A. S. (1975) *Nature 257*, 564−566.
41. Mas, M. T., and Colman, R. F. (1984) *Biochemistry 23*, 1675−1683.

42. Sem, D. S., and Kasper, C. B. (1993) *Biochemistry 32*, 11539−11547.
43. Steyn-Parve, E. P., and Beinert, H. (1958) *J. Biol. Chem. 233*, 843−849.
44. Cleland, W. W. (1977) *Adv. Enzymol. Relat. Areas Mol. Biol. 45*, 273−387.
45. Hyde, E. I., Birdsall, B., Roberts, G. C., Feeney, J., and Burgen, A. S. (1980) *Biochemistry 19*, 3746−3754.
46. Eyschen, J., Vitoux, B., Rahuel-Clermont, S., Marraud, M., Branlant, G., and Cung, M. T. (1996) *Biochemistry 35*, 6064−6072.
47. Porter, T. D., and Kasper, C. D. (1986) *Biochemistry 25*, 1682−1687.
48. Karplus, P. A., Daniels, M. J., and Herriott, J. R. (1991) *Science 251*, 60−66.
49. Sem, D. S., and Kasper, C. B. (1993) *Biochemistry 32*, 11548−11558.
50. Draper, R. D., and Ingraham, L. L. (1968) *Arch. Biochem. Biophys. 125*, 802−808.
51. Theorell, H., and Nygaard, A. P. (1954) *Acta Chem. Scand. 8*, 1649−1653.

BI010947T